



## CRISPR-Cas9 genome editing reveals that the *Pgs* gene of *Fusarium circinatum* is involved in pathogenicity, growth and sporulation

Alida van Dijk<sup>a,\*</sup>, Andi M. Wilson<sup>a,b</sup>, Bianke Marx<sup>a</sup>, Bianca Hough<sup>a</sup>,  
Benedicta Swalarsk-Parry<sup>a</sup>, Lieschen De Vos<sup>a</sup>, Michael J. Wingfield<sup>a</sup>, Brenda D. Wingfield<sup>a</sup>,  
Emma T. Steenkamp<sup>a</sup>

<sup>a</sup> Department of Biochemistry, Genetics and Microbiology (BGM), Forestry and Agricultural Biotechnology Institute (FABI), University of Pretoria, Pretoria, South Africa

<sup>b</sup> Section for Organismal Biology, Department of Plant and Environmental Sciences, University of Copenhagen, Denmark

### ARTICLE INFO

#### Keywords:

Pathogenicity  
Growth  
Sporulation  
*Pgs* gene  
*Fusarium circinatum*  
CRISPR-Cas9 genome editing

### ABSTRACT

*Fusarium circinatum*, the causal agent of pine pitch canker, is one of the most destructive pathogens of *Pinus* species worldwide. Infections by this pathogen result in serious mortality of seedlings due to root and root collar disease, and growth reduction in trees due to canker formation and dieback. Although much is known about the population biology, genetics, and genomics of *F. circinatum*, relatively little is known regarding the molecular basis of pathogenicity in *F. circinatum*. In this study, a protoplast-based transformation using CRISPR-Cas9-mediated genome editing was utilized to functionally characterize a putative pathogenicity gene in three different strains of the fungus. *In silico* analyses suggested the gene likely encodes a small secreted protein, and all isolates in which it was deleted displayed significantly reduced vegetative growth and asexual spore production compared to the wild-type isolates. In pathogenicity tests, lesions induced by the deletion mutants on detached *Pinus patula* branches were significantly shorter than those produced by the wild-types. The putative pathogenicity gene was named *Pgs* reflecting its role in pathogenicity, growth, and sporulation. Future research will seek to explore the molecular mechanisms underlying the mutant phenotypes observed. Overall, this study represents a significant advance in *F. circinatum* research as the development and application of a Cas9-mediated gene deletion process opens new avenues for functional gene characterization underlying many of the pathogen's biological traits.

### 1. Introduction

*Fusarium circinatum* (Nirenberg and O'Donnell, 1998) is the causal agent of pine pitch canker, one of the most destructive pathogens of *Pinus* species globally (Wingfield et al., 2008). It is thought to have originated in Mexico and the Caribbean, and subsequently spread to many countries, posing a significant threat to natural forests and plantation forestry (Drenkhan et al., 2020). The fungus can infect all life stages of *Pinus* plants, causing symptoms ranging from root and collar disease in seedlings to resinous cankers and dieback in mature trees (Wingfield et al., 2008). As a result, disease epidemics almost always have negative economic impacts due to yield loss and reduction in timber quality (Mitchell et al., 2011; Wingfield et al., 2008).

Many *Pinus* species can be infected by *F. circinatum*, with some displaying higher levels of disease tolerance (e.g., *P. caribaea* and

*P. oocarpa*) and others being highly susceptible (e.g., *P. radiata* and *P. patula*) to disease (Hodge and Dvorak, 2000; Mitchell et al., 2011). The basis of these differences in susceptibility is not well understood, although transcriptomic data point to an important role for early and efficient phytohormone signaling in the host plant (Visser et al., 2019). Infection by *F. circinatum* can also trigger systemic induced resistance in the host (Gordon et al., 2011), but the molecular basis for this remains unclear (Amaral et al., 2022).

The life history traits in *F. circinatum* further complicate investigations into its relationship with the host plant. For example, the pathogen can colonize the intercellular spaces of *Pinus* roots and live as an endophyte without causing any signs of disease (Martín-Rodríguez et al., 2015; Swett et al., 2016), but the reasons for a switch to necrotrophy and symptom development are not understood (Swett et al., 2016). Knowledge of the molecular basis of the interaction between

\* Corresponding author.

E-mail address: [alida.vandijk@up.ac.za](mailto:alida.vandijk@up.ac.za) (A. van Dijk).

<https://doi.org/10.1016/j.fgb.2025.103970>

Received 5 June 2024; Received in revised form 16 December 2024; Accepted 11 February 2025

Available online 12 February 2025

1087-1845/© 2025 The Authors. Published by Elsevier Inc. This is an open access article under the CC BY-NC-ND license (<http://creativecommons.org/licenses/by-nc-nd/4.0/>).

*F. circinatum* and its *Pinus* host is therefore crucial for developing strategies to combat and mitigate the destructive capacity of this pathogen.

One of the main hurdles to deciphering the molecular basis of traits in non-model fungi is the availability of gene knockout/modification systems for the functional characterization of target genes (Amselem et al., 2011; Zheng et al., 2017). In *F. circinatum*, the two main approaches that have been used for this purpose involve *Agrobacterium tumefaciens*-mediated transformation (ATMT) of conidia (Covert et al., 2001) and polyethylene glycol (PEG)-mediated transformation (PMT) of protoplasts (Phasha et al., 2021a, 2021b). Apart from allowing for the characterization of genes involved in *F. circinatum* pathogenicity, studies employing ATMT and PMT have also provided some knowledge regarding the genetic mechanisms determining traits such as the production of secondary metabolites (Muñoz-Adalia et al., 2018; Phasha et al., 2021a, 2021b). Although, RNA guided genome editing with CRISPR (clustered regularly interspaced short palindromic repeats)-Cas (CRISPR associated protein) 9 has not yet been applied to the pitch canker pathogen, applications based on this methodology are increasingly widely adopted for gene deletion due to its simplicity, affordability, and efficiency (Shinkado et al., 2022; Wang and Coleman, 2019a).

A widely used CRISPR-Cas9 strategy in *Fusarium* species involves utilizing pre-assembled CRISPR-Cas9 ribonucleoprotein (RNP) complexes (Ferrara et al., 2019; Lightfoot and Fuller, 2019; Pokhrel et al., 2022). Such a complex consists of the Cas9 nuclease bound to a synthetically produced single-guide RNA (sgRNA) that directs the complex to the target DNA site, where Cas9 introduces a double stranded break (Jinek et al., 2012). In the presence of donor DNA (dDNA), Cas9-mediated DNA cleavage triggers the cell's homology directed DNA repair mechanism, using the dDNA as the repair template (Doudna and Charpentier, 2014). In some *Fusarium* studies, the need for commercially available Cas9 and synthetically produced sgRNA have been eliminated by expressing these elements *in vivo* from expression cassettes on plasmids or integration into the genome of the fungus (Wang and Coleman, 2019a). However, development of these can be difficult (Song et al., 2019) and the relevant expression vectors and isolates are not available for *F. circinatum* or any of its close relatives.

The aim of this study was to functionally characterize a putative pathogenicity gene in *F. circinatum* using pre-assembled CRISPR-Cas9 RNP complexes to generate knockout mutants. For this purpose, multiple field-collected wild-type strains, together with their respective mutants, were subjected to pathogenicity tests, as well as growth and sporulation assays. The findings of this study would thus improve our understanding of pathogenicity in *F. circinatum*, while also expanding the molecular toolbox available for the fungus by providing a more effective and efficient method for genome editing.

## 2. Methods and materials

### 2.1. Isolates, routine culturing, and DNA extraction

Three isolates of *F. circinatum* (CMWF350, CMWF24 and CMWF1807) were used in this study and have all been preserved in the *Fusarium* culture collection (CMWF) of the Forestry and Agricultural Biotechnology Institute (FABI), University of Pretoria, South Africa. Isolate CMWF350 (FSP34) was obtained from diseased *Pinus* tissue in California and has whole genome sequence data (De Vos et al., 2024; Wingfield et al., 2018). Isolate CMWF24 (FCC1035) originated from a diseased *P. patula* seedling collected in the Mpumalanga province of South Africa (Santana et al., 2016), while isolate CMWF1807 was obtained from the leading edge of a canker collected from a 10-year-old *P. greggii* plantation tree in the KwaZulu-Natal province of South Africa (Fru et al., 2017).

The isolates were routinely grown for 7 days at 25 °C in 90 mm Petri dishes containing Potato Dextrose Agar (PDA) medium (Becton, Dickinson and Company, Franklin Lakes, NJ, USA), supplemented with 300

mg/l of Streptomycin sulfate salt (Sigma-Aldrich, Mannheim, Germany). DNA extractions were done as previously described (Phasha et al., 2021b).

### 2.2. In silico characterization of a putative pathogenicity gene

The gene targeted in this study emerged from a preliminary genome wide association study (Swalarsk-Parry et al., unpublished). The sequence data and the inferred amino acid sequence data for this gene were compared using BLASTn and BLASTp analyses to those in the databases of the National Center for Biotechnology Information (NCBI; <https://blast.ncbi.nlm.nih.gov/>) as well as MycoCosm (Grigoriev et al., 2014). To identify functionally important domains and conserved sites, sequences were analyzed using the online version (<https://www.ebi.ac.uk/interpro/search/sequence>) of InterProScan (Jones et al., 2014). Whether the gene encodes for a protein with signal peptide was investigated using SignalP 6.0 (Teufel et al., 2022), while EffectorP 3.0 (Sperschneider and Dodds, 2022) was used to determine whether the protein could represent an effector. The predicted protein was also examined using the Bologna Unified Subcellular Component Annotator (BUSCA) online tool (Savojarado et al., 2018). The transcriptome data produced in a previous *in planta* study of the *F. circinatum*-*Pinus* interaction (Visser et al., 2019) were used to determine whether the gene was expressed.

### 2.3. Design, synthesis and testing of sgRNA

The sgRNA was designed to specifically target the gene of interest as described previously (Wilson and Wingfield, 2020). It consisted of a protospacer region (20 nucleotides, nt) complementary to a region in the target gene and a 76-nt scaffold region to which Cas9 binds (Fig. 1). Potential protospacer regions were identified manually by searching for 5' NGG 3' sequence triplets within the target gene. These were annotated as protospacer adjacent motifs (PAM) (Wilson and Wingfield, 2020). The identified PAM and protospacer sequences were then compared to the remainder of the genome sequence using a BLASTn search implemented in CLC Main Workbench V 21.0.3 (Kim et al., 2013). This was to ensure that the potential protospacers did not have similarity outside the target gene, thus reducing the possibility of off-target effects of Cas9. Additionally, the combined protospacer and scaffold sequence, without the PAM sequence, was analyzed using the RNAfold WebServer included in the Vienna RNA Websuite (Gruber et al., 2008). This step was taken to verify that the sgRNA folds into the correct 3D structure for the Cas9 enzyme to bind effectively (Fig. 1).

The sgRNA was synthesized using the EnGen® sgRNA Synthesis Kit, *Streptococcus pyogenes* (New England Biolabs Inc.). In short, a T7 promoter sequence (5' TTCTAATACGACTCACTATAG 3') was added to the 5' end of the protospacer and a kit-specific sequence (5' GTTTA-GAGCTAGA 3') was added to the 3' end. The 5' and 3' amended protospacer oligonucleotide was synthesized by Inqaba Biotec and used to generate the full length sgRNA as per the manufacturer's protocol. The synthesized sgRNA was visualized by electrophoresis in 1× TAE (40 mM Tris-acetate, 2 mM EDTA, pH 8.5) buffer on 1 % (w/v) agarose (Sea-Kem®) gels with GelRed® Nucleic Acid Gel Stain (Biotium). The sgRNA was purified using the Monarch® RNA Cleanup Kit (New England Biolabs Inc.) and quantified using the Qubit™ RNA Assay Kit (Thermo Scientific™) as per the manufacturer's protocol.

The formation and cleaving capacity of the RNP complex were evaluated to ensure that the sgRNA would be effective in guiding the Cas9 to the target gene, and that DNA cleavage occurs upstream of the PAM sequence, within the complementary region. To perform these tests, the synthesized sgRNA and the *S. pyogenes* Cas9 nuclease, EnGen® Spy Cas9 NLS (New England Biolabs Inc.) was used as per the manufacturer's protocol. Briefly, 30 nM sgRNA and 30 nM Cas9 were pre-incubated in the presence of NEBuffer™ 3.1 for 10 min at 25 °C. A total of 3 nM of the DNA target was then added to the mixture, followed

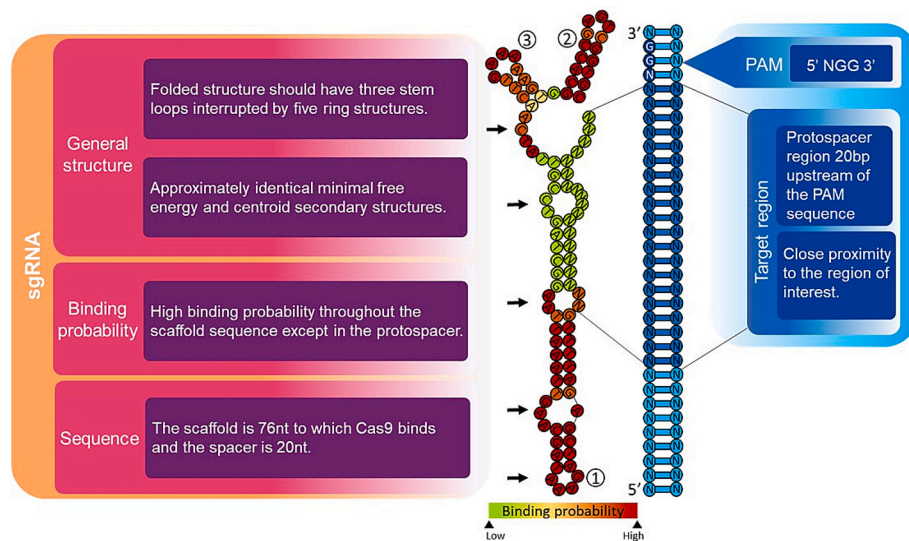


**Fig. 1.** Secondary folding structure of the single-guide RNA (sgRNA) for targeted Cas9 mediated editing. The scaffold region (76 bp) is pictured in red, and the protospacer in green (20 bp). The sgRNA structure requires three stem loops (numbered 1–3) and five interrupting rings (indicated in arrows). The dsDNA target region is on the left in blue. The protospacer region is the 20 bp upstream of the 5'NGG3' PAM (protospacer adjacent motifs) sequence (Wilson and Wingfield, 2020). (For interpretation of the references to colour in this figure legend, the reader is referred to the web version of this article.)

by incubation at 37 °C for 15 min. The DNA target was obtained using a touchdown PCR approach using the Phusion High-Fidelity PCR Master Mix with HF Buffer (Thermo Scientific™) and primers FCPPFTR and FCPPRTR (Table S1 and S2). The DNA target was cleaned using Sephadex® G-50 (Sigma-Aldrich) and quantified using a Qubit™ DNA Assay Kit as per the manufacturer’s protocol. Cleavage of the PCR product by the RNP complex was visualized using agarose gel electrophoresis as above, where two smaller bands were expected to be seen in comparison to the larger intact target region.

2.4. Design and synthesis of dDNA

The dDNA used in this study was designed to mediate replacement of the target gene with a sequence coding for the hygromycin B resistance gene cassette (Fig. 2). To achieve this, the dDNA fragment was designed to contain a 5' flanking region homologous to the genomic region upstream of the target gene, followed by the resistance cassette, and ending with a 3' flanking region homologous to the genomic region downstream

of the target gene. For this purpose, the 5' and 3' flanking regions were amplified with touchdown PCR (Table S2) using the Phusion High-Fidelity PCR Master Mix with HF Buffer and with primers FCPP5F, FCPP5RHYGF and FCPP3FHYGR, FCPP3R3, respectively (Tables S1). The reverse primer for the 5' flank and the forward primer for the 3' flank had additional sequences of ca. 25 nt that overlapped with the 5' and 3' respective sequences at the ends of the hygromycin B resistance gene cassette (Fig. 2).

Primers HygF and HygR (Tables S1 and S2) were used to amplify the hygromycin B resistance cassette from the pCB1004 plasmid which was extracted from *Escherichia coli* (Carroll et al., 1994) using the QIAGEN Plasmid Mini Kit following the manufacturer’s protocol. Amplicons were cleaned with Sephadex® G-50 and sequenced using the BigDye Terminator Cycle Sequencing Kit v3.1 (Life Technologies) and AB13100 Automated Capillary DNA sequencer (Thermo Fisher Scientific) at the Sequencing Facility of the University of Pretoria (Pretoria, South Africa).

An overlap extension PCR (Table S3) was performed using Long-Amp® Taq 2× Master Mix (New England Biolabs Inc.) to join all three

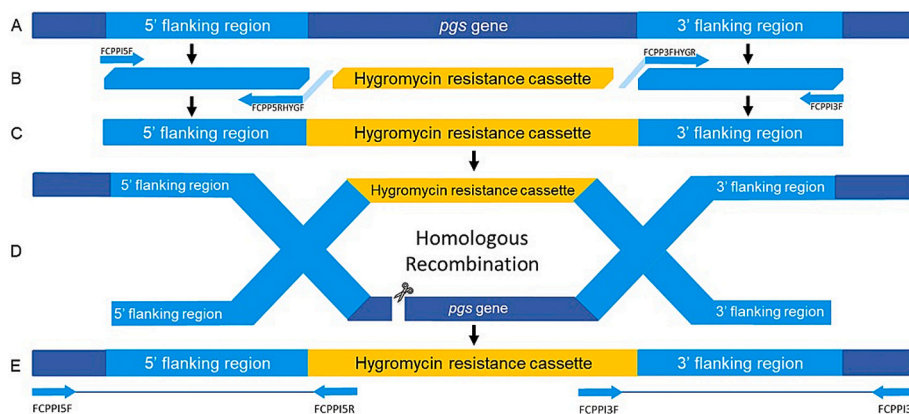


**Fig. 2.** Synthesis of the donor DNA using an overlap extension PCR and homology directed DNA repair (HDR). A: The genomic region containing the gene to be deleted and its flanking regions. B: The amplified 5' and 3' flanking regions with overhang primers matching sequence from the hygromycin B resistance cassette. C: The fully assembled dDNA fragment. D: HDR to mend the double stranded DNA produced by Cas9. The HDR is facilitated by homologous recombination of the identical flanks. E: Integration of the hygromycin B resistance cassette into the intended genomic region. The light blue arrows depict primers that were used to confirm integration of the dDNA within the intended genomic region. (For interpretation of the references to colour in this figure legend, the reader is referred to the web version of this article.)

components into the dDNA fragment in a single reaction (Zhao et al., 2019). The 5' flank forward primer (FCPP5F) and the 3' flank reverse primer (FCPP3R3) were the only primers added, as the overlap regions attached to the 3' end and 5' end of the 5' flank and 3' flank, respectively, acted as primers for the hygromycin B resistance cassette (Fig. 2B). The assembled dDNA fragment was visualized by electrophoresis as above using the Lambda DNA/EcoRI + HindIII Marker 3 ladder (Thermo Scientific). Amplicons were cleaned as before and then subjected to long read Sanger sequencing in a primer walking approach, using primers FCPP5F, HygF, HygR and FCPP3R3 (Table S1) to obtain overlapping sequence reads for the ca. 900 base pair (bp) fragment.

## 2.5. Protoplast preparation and transformation

Protoplasts were prepared from *F. circinatum* isolates CMWF350, CMWF24 and CMWF1807 as described previously (Phasha et al., 2021a, 2021b), but with modifications. In short, the isolates were inoculated in 400 ml Potato Dextrose Broth (PDB; Difco Laboratories, Detroit, MI) and incubated for 5 days at 25 °C on an orbital shaker (3 g). Cultures were filtered through two layers of Miracloth (Merck Millipore), after which filtrates were centrifuged (4000 g) for 20 min at 4 °C to harvest conidia. Pelleted conidia were resuspended in 100 ml of sterile Yeast Peptone Dextrose (YEPD) broth containing 3 g/l yeast extract (Difco Laboratories), 1 g/l Bacto™ peptone (Difco Laboratories), and 20 g/l dextrose. After orbital shaking (3 g) for 10 h at 25 °C, cultures were again filtered through two layers of Miracloth and centrifuged (4000 g) for 20 min at 4 °C to pellet the germinating conidia. The latter were resuspended in protoplasting buffer containing 40 ml KCl, 1 g Driselase from Basidiomycetes (Sigma Chemical Co., St. Louis; D8037), 2 mg Chitinase from *Streptomyces griseus* (Sigma Chemical Co., St. Louis; C6137) and 200 mg lysing enzyme from *Trichoderma harzianum* (Sigma Chemical Co., St. Louis; L1412). The mixture was then incubated on an orbital shaker (1 g) at 30 °C. The progress of the digestion was viewed under a light microscope at hourly intervals.

After 2–6 h, the digestion solution was filtered through three layers of Miracloth and centrifuged (3000 g) for 5 min at 4 °C. The supernatant was discarded, the pelleted protoplasts were resuspended in 10 ml of STC (1.2 M Sorbitol, 10 mM Tris-HCl pH 8, 50 mM CaCl<sub>2</sub>) buffer and centrifuged as before. The supernatant was again discarded, and the pellet resuspended in 1 ml STC and centrifuged (3500 g) for 5 min at 4 °C. This step was repeated, and the pellet was resuspended in a final volume of 300–600 µl STC buffer. The protoplasts were quantified using a hemocytometer (Neubauer Improved Brightline) with an expected yield of 10<sup>6</sup>–10<sup>8</sup> protoplasts/ml (Fig. S1).

Transformation reactions were prepared in 50 ml Falcon™ tubes using protoplast suspensions, freshly prepared, pre-assembled RNP complex, and dDNA. The RNP complex was assembled by incubating 3 µM sgRNA and 3 µM EnGen® Spy Cas9 NLS for 10 min at 25 °C in NEBuffer™ 3.1. Each transformation reaction contained 100 µl of the protoplast suspension, 100 µl STC buffer, 12.5 µl RNP complex and 6 µg dDNA in the presence of 30 % (w/v) PEG 8000 (Sigma-Aldrich). Reactions were incubated at room temperature for 10 min, after which 4 ml STC buffer was added and mixed by gentle inversion. Lastly, 9 ml of regeneration medium (RM) was added to the mixture, followed by overnight incubation on an orbital shaker (3 g) at room temperature. The RM consisted of 271 g/l sucrose; 1 g/l yeast extract; 1 g/l N-Z-Amine AS (Sigma-Aldrich).

To select for putative transformants, 1.4 ml of the transformation reaction was decanted into 65 mm Petri dishes. A thin layer of selection medium (SM; identical to RM but containing 12 g/l agar) supplemented with 100 µg/ml hygromycin B from *Streptomyces hygroscopicus* (Sigma-Aldrich) was added to the Petri dish and mixed with gentle swirling. After the SM solidified, another layer of SM, this time supplemented with 150 µg/ml of hygromycin B, was added (Phasha et al., 2021a, 2021b).

Potential transformants (i.e., those that grew through both layers of

hygromycin B-supplemented SM), were screened by PCR using hyR and ygF primers nested within the hygromycin B resistance cassette (Table S1 and S2). Positive recombinants were further screened to confirm that the dDNA had integrated into the correct genomic position. For this purpose, primers FCPI5F and FCPI3R were designed to border the 5' and 3' flanking regions of the dDNA, while primers FCPI5R and FCPI3F were situated within the resistance cassette (Fig. 2E). PCR amplification was done using Phusion High-Fidelity PCR Master Mix with HF Buffer (Thermo Scientific™) (Table S1 and S2). Amplified fragments were cleaned and sequenced as before. The number of integrations was then assessed by Southern Blot analysis as described previously (Phasha et al., 2021a).

Isolates that were positive for the hygromycin resistance cassette but had been shown by PCR to have been integrated at a locus other than the target locus were also isolated and used as transformant controls. Therefore, transformant controls represented isolates that have undergone the same protoplasting and transformation procedures as the mutants, but where the hygromycin B resistance cassette had integrated elsewhere in the genome and did not disrupt the gene of interest. These control isolates were selected for by using SM supplemented with 150 µg/ml hygromycin B. To confirm random integration, PCRs with primers hyR and ygF as described above were done to confirm integration in the genome, while PCR of the target gene was done using FCPPFTR and FCPPRTR, as above, to confirm that the target gene was still intact (Table S1 and S2). To ensure phenotypic differences observed between the wild-type and knockout strains are not due to the transformation process, transformant controls were included in all assays.

## 2.6. Analysis of vegetative growth and sporulation

A study was conducted to assess the effect of the gene knockout on mycelial growth. For this purpose, conidia were harvested from 7-day old PDA cultures of the three wild-type, three knockout, and three transformant control isolates. This was done by washing the cultures with 20 % (v/v) glycerol solution, harvesting the conidia, and then quantifying the suspension with a hemocytometer. A 10 µl suspension of spores (5 × 10<sup>4</sup> spores/ml) was transferred to the center of each of three 90 mm Petri dishes containing PDA. For each isolate, three replicates were incubated at 25 °C in the dark for 7 days. Colony diameter was then recorded using the mean of two measurements taken along two perpendicular axes.

To assess the impact of gene knockout on conidium production, a conidial suspension was prepared by taking a 10 mm diameter plug from the leading edge of mycelial growth on a 7-day-old PDA culture. The plug was added to a cryotube containing 1.5 ml of 20 % (v/v) glycerol and agitated thoroughly in a vortex mixer, after which the number of spores in the suspension was quantified using a hemocytometer. This was done three times, with plugs taken from different locations on the same plate (three technical repeats). For each isolate, the entire procedure was conducted using three separate 7-day-old PDA cultures, thus providing three biological repeats.

Conidial germination was assessed by plating 1 ml of the spore suspension (5 × 10<sup>4</sup> spore/ml) onto 90 mm Petri dishes containing PDA. These were incubated at 25 °C for 12 h in the dark and visualized under a microscope to assess whether germination time was affected by the gene knockout. Three replicate assessments were made for each isolate. A block of agar was excised from the plate and a coverslip was placed over it and visualized under a light microscope. The lengths of the germ tubes emerging from the conidia were measured for each of the isolates.

Microscopic features such as the formation of sporodochia and types of spores of the various isolates were also examined. For this purpose, all isolates were inoculated onto Petri dishes containing PDA and pieces of sterile carnation leaves (Phasha et al., 2021b). Plates were incubated at 25 °C under a 12/12-h near-UV light/dark cycle. Microscopic observations were then made at 63× magnification under a light microscope using a standard slide and water as a mounting medium.

## 2.7. Pathogenicity assays

Aggressiveness, the quantitative component of pathogenicity (Pariaud et al., 2009), of the wild-type, knockout, and transformant control isolates was assessed by inoculating freshly detached branches collected from 3-year-old *P. patula* trees grown in a plantation in Jes-sievale, Mpumalanga Province, South Africa (26°09'47.1"S 30°24'24.1"E). Healthy branches of ca. 14 mm in diameter were taken from the lower whorls of the trees and cut to ca. 174 mm lengths by selecting regions between whorls. The cut ends of branch sections were immediately dipped in molten paraffin wax to prevent desiccation. A total of 10 branches were collected per tree, from 30 trees. In the pathogenicity assay, each isolate was inoculated onto a branch obtained from a different tree. This meant that all 9 isolates and a negative control were inoculated per tree, yielding 30 replicates (Table S4).

For inoculation, a sterile 10 mm cork borer was used to expose the sapwood in the middle of the branch. The same sterile cork borer was then used to remove a 10 mm mycelial plug from the actively growing margin of a 7-day-old culture grown on PDA supplemented with 300 mg/l of Streptomycin sulphate salt (Sigma-Aldrich). The plug was placed into the wound on the branch with the mycelium-side facing the sapwood, and then kept in place with parafilm. For the negative control, a sterile PDA plug was used. The inoculated branches were incubated at 25 °C for 21 days in open containers. The bark was then peeled back to reveal the lesion in the sapwood and cambium layer, which were measured with vernier calipers along the length of the branch. To normalize for potential variation linked to branch thickness, lesion lengths were recorded as the measured length (mm) of the lesion divided by the width (mm) of the branch. The entire pathogenicity trial was repeated using the same methods and materials. The first trial was conducted in April 2023, while the second trial was conducted in July 2023.

To confirm that the lesions were caused by *F. circinatum*, isolations were done from the leading edges of the lesions. From the resulting 7-day-old culture, DNA was extracted using PrepMan™ Ultra Sample Preparation Reagent (Thermo Scientific™). These DNAs were used as templates in PCRs with the diagnostic CIRC1 and CIRC4 primers (Table S1) as previously described (Schweigkofler et al., 2004). Knockout isolates and transformant control isolates were confirmed via PCR with primers HygF and HygR (Table S1 and S2).

## 2.8. Data analysis

Analysis of variance (ANOVA) was used to compare the means recorded for the wild-type, knockout, and transformant control isolates (as well as the negative controls in case of the pathogenicity assays). Tukey's Honestly Significant Difference (HSD) tests were used to determine which groups were significantly different from each other (Christensen, 1997). All ANOVAs and Tukey's HSD tests were performed using the online tools available at [https://astatsa.com/OneWay\\_Anova\\_with\\_TukeyHSD/](https://astatsa.com/OneWay_Anova_with_TukeyHSD/).

## 3. Results

### 3.1. In silico characterization of a putative pathogenicity gene

Comparison of the coding sequence of a putative pathogenicity gene examined in this study against the transcriptome data previously produced from *F. circinatum*-infected *Pinus* tissue showed that expression of the gene was upregulated *in planta* (Visser et al., 2019). SignalP analysis suggested that the predicted protein contains a signal peptide. It reported a probability score of 0.9989 that the first 24 aa at the N-terminus of the inferred protein represents a signal peptide that typically targets a protein to the secretory pathway (Teufel et al., 2022). Analysis with BUSCA suggested that the mature protein is likely (prediction score = 1) secreted because it was assigned the "extracellular space" Gene

Ontology (GO) term with GO number 0005615 (Binns et al., 2009). EffectorP predicted with 0.75 probability that the protein represents an apoplastic effector, i.e., a protein secreted into the space outside the plasma membrane of plant tissues (De Wit, 2016). These predictions were corroborated with InterProScan, which annotated the first 24 residues as a signal peptide, and the remainder of the protein as a "non-cytoplasmic" domain. No other conserved domains were detected with InterProScan.

Comparison of the nucleotide sequence of the coding region and the inferred protein sequence of the target gene against those in the NCBI database showed high similarity (>96 %) to genes annotated as a "pathogenicity protein" in *F. circinatum* (accession number KAF5663390) and in *Fusarium subglutinans* (accession number XM\_036676922.1). Both genes were annotated *in silico* in a previous genomics study without supporting experimental evidence of gene function (Kim et al., 2020). The same was true for most of the remaining BLAST hits. Similar results were obtained using MycoCosm's BLAST tool, with the only exception being gene FGSG\_07755 in *Fusarium graminearum* for which additional information was available. It shared 89,4 % mRNA and 89,3 % protein sequence identity with the *F. circinatum* target gene and was previously shown to be involved during the infection of wheat by *F. graminearum* (Hoang, 2017).

### 3.2. Deletion mutants and transformant controls

The sgRNA targeted a region 66 nt from the first nucleotide in the target gene. The RNP complex prepared by combining this sgRNA with EnGen® Spy Cas9 NLS cleaved the targeted double stranded DNA region as expected. This was evidenced by the production of two distinct bands corresponding to 66 bp and 412 bp from the intact 478 bp amplicon. In the presence of dDNA, the pre-assembled RNP complex also mediated efficient replacement of the target gene with the hygromycin B resistance cassette because transformation of the *F. circinatum* protoplasts yielded numerous putative transformants. Although capable of growing on PDA supplemented with 150 µg/ml hygromycin B, PCRs with primers FCPPI5F, FCPPI5R, FCPPI3F and FCPPI3R were used to confirm integration of the cassette in the correct position in transformants from all three isolates. For each of the three wild-type isolates, a transformant control isolate was also isolated, where the dDNA integrated elsewhere in the genome without disrupting the target gene. Southern blot analysis confirmed single-copy integrations for all knockout isolates and transformant control isolates.

### 3.3. Vegetative growth and sporulation

Colony morphology and sporodochia formation, as well as the shape and size of conidia were similar among isolates, regardless of their genotype (Fig. 3 and Fig. S2). The conidia of all isolates also germinated after ca. 12 h of incubation at 25 °C, suggesting a limited impact of the gene knockout on these properties. However, differences in pigmentation were seen in the cultures, with the wild-type strains and transformant controls appearing more purple than the pale knockout mutants. Also, the isolates all produced aerial hyphae, but the knockout isolates appeared to have a slightly increased number of aerial hyphae compared to the wild-type and transformant controls. The growth assay further showed that the knockout mutants for the three *F. circinatum* strains all produced significantly smaller ( $p < 0.1$ ) colonies on PDA following incubation at 25 °C for 7 days (Fig. 3). Their mean colony diameter ranged from 32 mm to 39 mm compared to the 48 mm to 54 mm for the wild-type strains (Fig. 3B). Mean colony diameters recorded for the transformant controls did not differ significantly from those of the wild-type strains. Similarly, conidium production was significantly ( $p < 0.01$ ) decreased in the knockout mutants compared to the transformant controls and wild-type isolates (Fig. 4), with the wild-type strains producing similar numbers of conidia as the transformant controls.

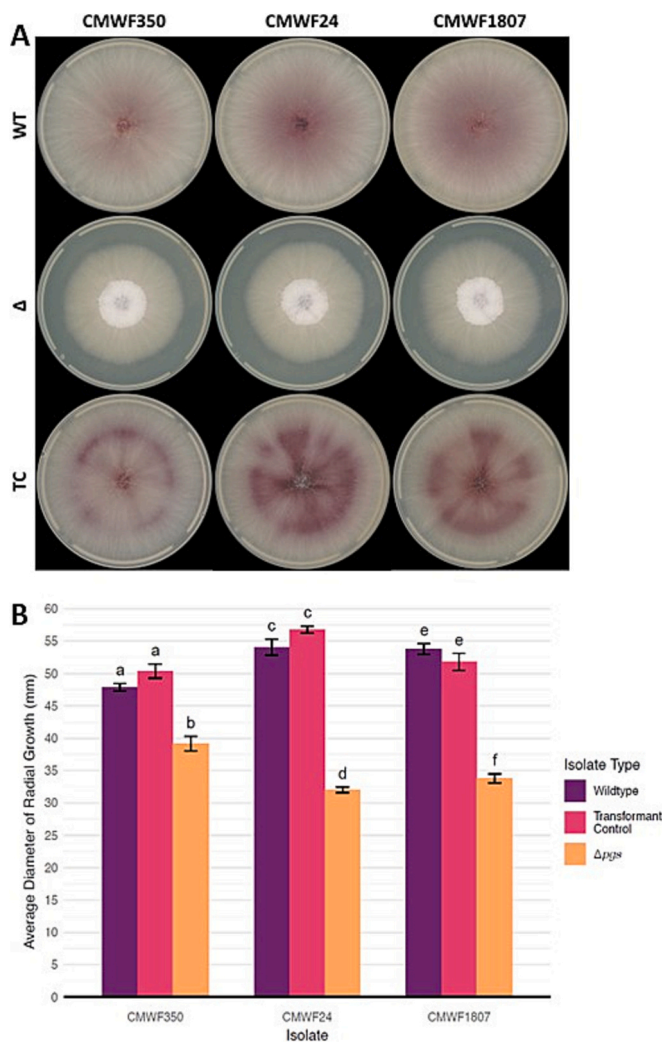


**Fig. 3.** Mycelial growth comparisons of the wild-type (WT), knockout strain ( $\Delta$ ) and transformant control (TC) of isolates CMWF350, CMWF24 and CMWF1807 of *F. circinatum*. A: After 7 days of incubation at 25 °C in the dark on PDA, the WT and TC isolates showed little difference, but both produced significantly ( $p < 0.001$ ) larger colonies than the  $\Delta$  strains. B: Average colony diameter of the respective isolates after 7 days of growth at 25 °C in the dark on potato dextrose agar medium. For each set of results (i.e., those for a wild-type isolate and its corresponding deletion mutant and transformant control), significant differences among means are shown with different letters (a to f) above the bars depicting standard deviation.

### 3.4. Pathogenicity assays

The knockout mutants were significantly less aggressive ( $p < 0.1$ ) than the transformant controls and wild-type isolates in the assay using detached *Pinus* branches (Fig. 5). The lesions caused by the three knockout mutants ranged in length from 1,2 mm to 4,8 mm relative to the 5,0–6,9 mm lesions produced by the wild-type strains. The lesion lengths induced by the wild-type isolates did not differ significantly from the transformant control isolates. For the control treatment, in which detached *Pinus* branches were inoculated with sterile PDA, no lesion development was observed (Fig. 5). PCR with the *F. circinatum*-specific primers of fungi re-isolated from the lesions (and sequencing of a portion of the hygromycin B resistance cassette for the mutants) confirmed that the lesions were caused by the same isolates used in the inoculations.

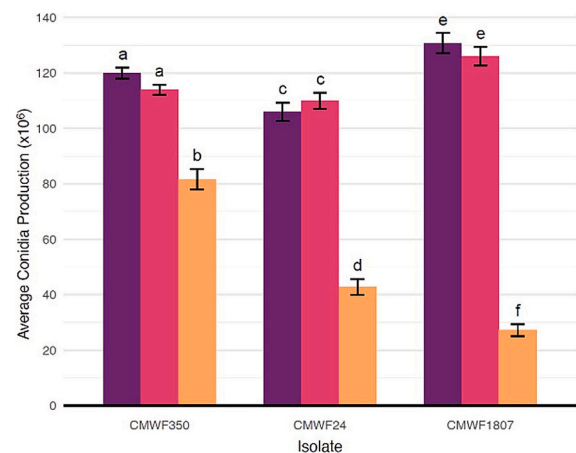


**Fig. 4.** Comparisons of sporulation of the three *F. circinatum* wild-type isolates and their corresponding mutant and transformant control isolates. Average spore counts recorded for the respective fungal isolates. For each set of results (i.e., those for a wild-type isolate and its corresponding deletion mutant and transformant control), significant differences among means are shown with different letters (a to f) above the bars depicting standard deviation.

## 4. Discussion

A gene deletion process based on CRISPR-Cas9 in *F. circinatum* was developed and applied in this study. The target gene was knocked out in three isolates of the fungus and the deletion mutants were characterized using a range of phenotypic traits. All the knockout mutants showed significant reduction in comparison to their respective wild-type isolates with regards to the lesions induced on detached *P. patula* branches, vegetative growth, and the number of conidia produced. Accordingly, we propose that the putative pathogenicity gene characterized in this study be referred to as *Pgs* to reflect its involvement in pathogenicity, growth, and sporulation.

Our gene knockout system involved the *in vitro* combination of the Cas9 effector and sgRNA to form an RNP-complex, which was then combined with protoplasts for transformation. The use of *in vitro* pre-assembled RNPs is generally thought to be more advantageous than using transformation with plasmids encoding Cas9 and the relevant sgRNA, particularly because insufficient Cas9 expression and potentially random genomic integrations are avoided (Nagy et al., 2017; Wang et al., 2018a, 2018b; Wilson and Wingfield, 2020). Additionally, the introduction of Cas9 under a constitutive promoter into filamentous fungi using a plasmid-based approach could also lead to overexpression of Cas9, resulting in off-target effects over time (Nagy et al., 2017). In contrast, transformation using the RNP complex ensured that Cas9 was present at a precise concentration and ensured the rapid degradation of *in-vitro*-assembled RNPs minimized off-target effects by only exposing cells to Cas9 for a brief period (Kim et al., 2014).

Although pre-assembled RNPs have been used to generate gene knockouts in other species of *Fusarium* including *F. graminearum* (Lee et al., 2022), *Fusarium proliferatum* (Ferrara et al., 2019) and *Fusarium oxysporum* (Wang et al., 2018a, 2018b; Wang and Coleman, 2019b), it had not previously been done in *F. circinatum*. This is also the first report of using the CRISPR-Cas9 system to generate knockouts in *F. circinatum* as previous gene knockouts were generated with PMT of protoplasts using the split marker approach (Phasha et al., 2021a, 2021b) or ATMT coupled with the use of a deletion construct (Covert et al., 2001; Muñoz-Adalia et al., 2018). Indeed, the introduction of CRISPR-Cas9 knockout system as an RNP complex is advantageous over these previous systems as it avoids the lengthy and laborious process of designing and synthesizing the particular vectors required (Ullah et al., 2020). The CRISPR-Cas9-mediated gene knockout system developed in the present study expands the molecular toolbox available for *F. circinatum* and other

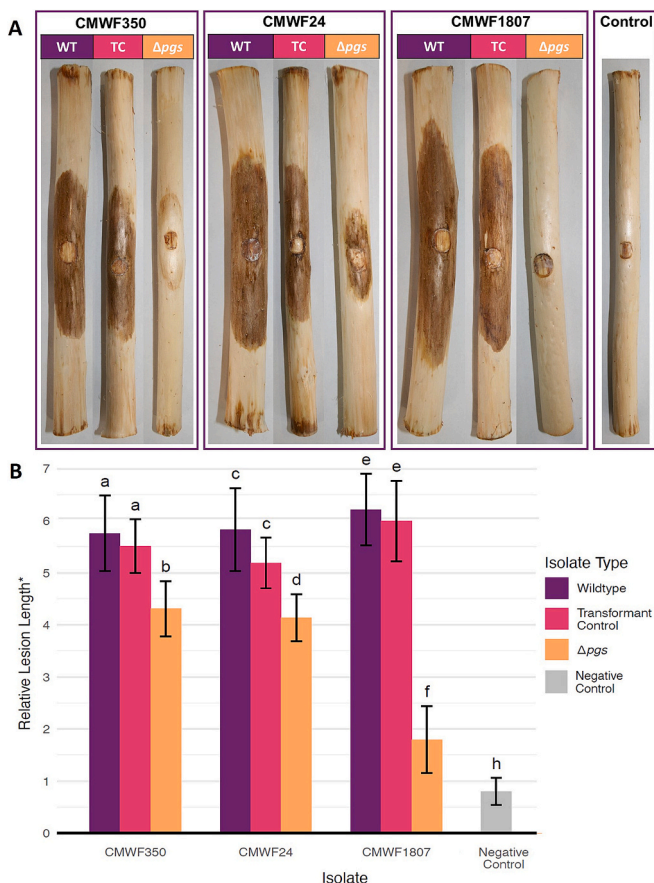


**Fig. 5.** Results of the pathogenicity assay conducted on detached branch sections collected from 3-year-old plantation trees of *P. patula*. A: The relative lesion length calculated as the average length of lesion (mm) on detached branch sections of *P. patula*, normalized by branch width (mm). For each set of results (i.e., those for a wild-type isolate and its corresponding deletion mutant and transformant control, as well as the negative control involving inoculation with sterile agar plugs), significant differences among means are shown with different letters above the bars depicting standard deviation. B: Examples of the lesions observed, which presented as brown discoloration in the cambium layer. (For interpretation of the references to colour in this figure legend, the reader is referred to the web version of this article.)

closely related species, providing an efficient method to functionally characterize genes involved in any number of biological processes.

To ensure the reliability of our gene deletion process, we created transformant control mutants with a fungicide resistance cassette integrated outside the targeted gene, serving as a baseline for comparative analyses. This approach avoided potential confounding effects arising from the insertion process or fungicide resistance. Unlike typical gene knockout studies using complementation mutants in which the disrupted gene is reintroduced using a second fungicide selection marker (Turgeon et al., 2010; Arras et al., 2015), our method minimized the risk of unintended genetic alterations or expression changes. For example, presence of the geneticin resistance cassette has been shown to deregulate translation of neighboring genes in knockout strains of *Saccharomyces cerevisiae* (Egorov et al., 2021), while off-target kinase activity of the phosphotransferase encoded by the hygromycin B resistance gene has been linked to altered virulence in *Histoplasma capsulatum* (Smulian et al., 2007). Therefore, to ensure experimental rigor, we produced *Pgs* knockout mutants for multiple wild-type *F. circinatum* strains and generated transformant control mutants to use as a basis for comparison during the phenotypic assays.

The results of the inoculation assay on detached *P. patula* branches provides evidence that the product of *Pgs* gene contributes to

pathogenicity and disease development in *F. circinatum*. The knockout strains for all isolates caused significantly shorter lesions compared to the wild-type isolates and the transformant controls. The *Pgs* homolog in *F. graminearum* (i.e., *FGSG\_07755*) was also putatively designated as a pathogenicity gene in a transcriptome study (Hoang, 2017). In that study, the *FGSG\_07755* gene appeared to be integral to the infection process as it was significantly upregulated during infection and exclusively expressed in the pathogen's infection cushions (Hoang, 2017). Likewise, *Pgs* was also significantly upregulated *in planta* in a previous transcriptome analysis of *F. circinatum*-infected *Pinus* tissue (Visser et al., 2019). However, to the best of our knowledge, the product of *FGSG\_07755* or any other homolog of *Pgs* has not yet been described or functionally characterized.

*In silico* analyses of the *F. circinatum Pgs* suggests that its protein product could represent an effector that is targeted to the secretory pathway and secreted into the extracellular space outside the plasma membrane of plant tissues (Savojarado et al., 2018; Sperschneider and Dodds, 2022; Teufel et al., 2022). The effectors secreted by fungi are typically involved in altering host-cell structure and function, facilitating infection, and triggering defense responses (Sperschneider et al., 2016; Wang et al., 2020). These small secreted proteins (SSPs), harboring a signal peptide and a sequence of less than 300 aa, have been shown to play important roles in niche colonization, nutrition, and virulence in fungi (Plett and Plett, 2022; Tanaka and Kahmann, 2021; Teulet et al., 2023). The results of this study provide strong justification for further research aimed at understanding the specific mechanisms associated with the *Pgs* gene and the role of its product in the pathogenicity of *F. circinatum* to *Pinus* species.

The *Pgs* gene was found to play a role in conidium production but was dispensable for the germination of these reproductive propagules. Conidia produced by the knockout mutants germinated at the same time as those of the wild-type and transformant control isolates. Compared to these isolates, however, the knockout mutants produced significantly fewer conidia. In other *Fusarium* species, various genes have been implicated in conidium development and production (Lu et al., 2023; Tang et al., 2020; Yang et al., 2023) of which some represent effectors or SSPs. In *Fusarium oxysporum*, for example, deletion of the *SIX9* (secreted in xylem 9) gene significantly reduced conidium production (Ayukawa et al., 2021), while knockout of SSPs such as FoSsp1 (a 145 aa uncharacterized protein) and FocCP1 (a cerato-platanin) apparently enhances conidiation (Liu et al., 2019; Wang et al., 2022). The decreased sporulation associated with *Pgs* deletion in the present study suggests that this gene affects the biological fitness of *F. circinatum*, as these propagules could be involved in dispersal and establishment of the pathogen in forests (Wingfield et al., 2008). This is because high rates of conidiation increase the potential for primary and secondary infections, driving polycyclic disease cycles and facilitating the spread of the pathogen to new host tissues or plants (Garbelotto et al., 2008; Dvořák et al., 2017). Future research should investigate the role of *Pgs* in conidial production and development under natural field conditions, especially when it infects and colonizes the *Pinus* host.

Deletion of the *Pgs* gene demonstrated that it has a role in vegetative growth and pigmentation of *F. circinatum* in culture, as all the knockout mutants were less pigmented and grew significantly slower than their respective wild-types and transformant controls. Reduced growth was previously also associated with mutants in which guanosine triphosphatase (GTPase)-encoding genes such as *Ras2* and *Fcrho1* were deleted (Phasha et al., 2021; Muñoz-Adalia et al., 2018). In terms of pigmentation, various previous studies illustrated the role of secondary metabolite biosynthesis genes for producing characteristic coloration in *Fusarium* cultures (Brown et al., 2012; Cambaza, 2018; Studt et al., 2012). In *F. verticillioides*, for example, deletion of certain genes needed for fumonisin biosynthesis yielded cultures that were more intensely purple than the wild-type strain, presumably due to stresses caused by the build-up of biosynthetic intermediates (Josselin et al., 2024). This is similar to that seen in *F. circinatum*, where disruption of fusaric acid

biosynthesis yields cultures with a reddish coloration, likely due to a feedback mechanism causing enhanced biosynthesis of bikaverin, another secondary metabolite (Phasha et al., 2021b). Disruption of these pathways and other secondary metabolite biosynthesis pathways also has been shown to yield pale or unpigmented *Fusarium* cultures (Rodríguez-Ortiz et al., 2013). Although little is known regarding the role of SSPs in the pigmentation and growth in culture of *Fusarium* species, these phenotypes have mostly been reported not to change in deletion mutants (Guo et al., 2022; Hao et al., 2020).

All of the identified phenotypes impacted by the deletion of *Pgs* in *F. circinatum* (i.e., aggressiveness, conidium production and vegetative growth) represent complex biological traits that are underpinned by multiple genes and molecular processes (Lannou, 2012). Such traits are increasingly also being shown in systems biology studies to be regulated by intricate gene networks (Wang et al., 2018). This is consistent with reports of certain genes having joint functions in pathogenicity, vegetative growth, and conidial production (Li et al., 2019; Liu et al., 2020; Xiong et al., 2019). In *F. circinatum*, for example, the Ras2 GTPase is essential for both pathogenicity and efficient growth in culture (Phasha et al., 2021a). Despite a general lack of correlation in mycelial growth and pathogenicity across populations of *F. circinatum* and other *Fusarium* species (Brennan et al., 2003; De Vos et al., 2011; Swalarsk-Parry et al., 2024), it is probable that these complex traits involve shared regulatory proteins and/or parts of pathways.

Given that these complex traits may have related underlying genetic mechanisms, we cannot discount the possibility that reduced growth and conidiation of the *Pgs* deletion mutants directly impacted the decreased levels of aggressiveness observed (Pariaud et al., 2009). Growth facilitates colonization and invasion of host tissues, with rapid growth often enabling the pathogen to outpace defense responses (Koeck et al., 2011), while conidiation contributes to this process by producing more infectious propagules (Drenkhan et al., 2020). In fact, a range of other potential developmental defects could have also caused the reduced lesion lengths observed for the *Pgs* deletion mutants (Pariaud et al., 2009; van der Does and Rep, 2017). Undoubtedly, detailed analyses of how *Pgs* mediates the phenotypic traits observed in this study would contribute significantly to our understanding of the pitch canker pathogen's developmental biology and interaction with its *Pinus* host.

## 5. Conclusions

This study represents a significant advancement in the field of *Fusarium* species research. The development and application of a Cas9-mediated gene deletion process in *F. circinatum* opens new avenues for functional gene characterization, particularly in the context of traits determining the pathogen's biological fitness. Successful knockout of the *Pgs* gene also provides a first glimpse as to how some of these traits might be impacted by a SSP, the function of which would be explored in our future research. The findings presented here also warrant research into the specific molecular mechanisms underlying the various fitness traits, especially as some might be correlated or associated with one another as reported in other fungi (Doohan et al., 2003; Kim et al., 2009; Luo et al., 2014). Undoubtedly, the application of CRISPR-Cas-based technologies, combined with conventional genetics approaches, will allow for a more detailed understanding of the molecular mechanisms and processes shaping the biological fitness of *F. circinatum*, as well as its interaction with *Pinus* species.

Supplementary data to this article can be found online at <https://doi.org/10.1016/j.fgb.2025.103970>.

## CRedit authorship contribution statement

**Alida van Dijk:** Writing – review & editing, Writing – original draft, Methodology, Investigation, Formal analysis, Data curation, Conceptualization. **Andi M. Wilson:** Writing – review & editing, Supervision,

Methodology, Conceptualization. **Bianke Marx:** Methodology. **Bianca Hough:** Methodology. **Benedicta Swalarsk-Parry:** Supervision, Methodology. **Lieschen De Vos:** Writing – review & editing, Supervision, Methodology. **Michael J. Wingfield:** Writing – review & editing, Supervision, Methodology, Conceptualization. **Brenda D. Wingfield:** Writing – review & editing, Supervision, Project administration, Funding acquisition. **Emma T. Steenkamp:** Writing – review & editing, Supervision, Project administration, Funding acquisition, Data curation, Conceptualization.

## Declaration of competing interest

The authors declare that they have no known competing financial interests or personal relationships that could have appeared to influence the research reported in this paper.

## Acknowledgments

We acknowledge the team at York timber for providing the *P. patula* trees for pathogenicity trials, Prof Tuan Duong for his assistance with the Southern Blot analyses, Dr. Neriman Yilmaz, Prof Cobus Visagie, Ms. Claudette Dewing and Ms. Nicole van Vuuren for their help with the microscopy and photography. This work was supported by funds from the Tree Protection Cooperative Programme (TPCP), the University of Pretoria, as well as the National Research Foundation (NRF) and Department of Science and Innovation (DSI) via their DSI-NRF Centre of Excellence in Plant Health Biotechnology (CPHB) and the DSI-NRF South African Research Chairs Initiative (SARChI) Chair in Fungal Genomics (Grant number: 98353). The grant holders acknowledge that opinions, findings and conclusions or recommendations expressed are those of the researchers and that the funding bodies accept no liability whatsoever in this regard.

## Data availability

Data will be made available on request.

## References

- Amaral, J., Valledor, L., Alves, A., Martín-García, J., Pinto, G., 2022. Studying tree response to biotic stress using a multi-disciplinary approach: the pine pitch canker case study. *Front. Plant Sci.* 13, 916138. <https://doi.org/10.3389/fpls.2022.916138>.
- Amsellem, J., Cuomo, C.A., van Kan, J.A.L., Viaud, M., Benito, E.P., Couloux, A., Coutinho, P.M., de Vries, R.P., Dyer, P.S., Fillinger, S., Fournier, E., Gout, L., Hahn, M., Kohn, L., Lapalu, N., Plummer, K.M., Pradier, J.-M., Quévillon, E., Sharon, A., Simon, A., ten Have, A., Tudzynski, B., Tudzynski, P., Wincker, P., Andrew, M., Anthouard, V., Beever, R.E., Beffa, R., Benoit, I., Bouzid, O., Brault, B., Chen, Z., Choquer, M., Collémare, J., Cotton, P., Danchin, E.G., Da Silva, C., Gautier, A., Giraud, C., Giraud, T., Gonzalez, C., Grossetete, S., Gildener, U., Henrissat, B., Howlett, B.J., Kodira, C., Kretschmer, M., Lappartient, A., Leroch, M., Levis, C., Mauceli, E., Neuvéglise, C., Oeser, B., Pearson, M., Poulain, J., Poussereau, N., Quesneville, H., Rasclé, C., Schumacher, J., Séguens, B., Sexton, A., Silva, E., Sirven, C., Soanes, D.M., Talbot, N.J., Templeton, M., Yandava, C., Yarden, O., Zeng, Q., Rollins, J.A., Lebrun, M.-H., Dickman, M., 2011. Genomic analysis of the necrotrophic fungal pathogens *Sclerotinia sclerotiorum* and *Borytis cinerea*. *PLoS Genet.* 7, e1002230. <https://doi.org/10.1371/journal.pgen.1002230>.
- Arras, S.D.M., Chitty, J.L., Blake, K.L., Schulz, B.L., Fraser, J.A., 2015. A genomic safe haven for mutant complementation in *Cryptococcus neoformans*. *PLoS One* 10, e0122916. <https://doi.org/10.1371/journal.pone.0122916>.
- Ayukawa, Y., Asai, S., Gan, P., Tsushima, A., Ichihashi, Y., Shibata, A., Komatsu, K., Houterman, P.M., Rep, M., Shirasu, K., Arie, T., 2021. A pair of effectors encoded on a conditionally dispensable chromosome of *Fusarium oxysporum* suppress host-specific immunity. *Commun Biol* 4, 707. <https://doi.org/10.1038/s42003-021-02245-4>.
- Binns, D., Dimmer, E., Huntley, R., Barrell, D., O'Donovan, C., Apweiler, R., 2009. QuickGO: a web-based tool for gene ontology searching. *Bioinformatics* 25, 3045–3046. <https://doi.org/10.1093/bioinformatics/btp536>.
- Brennan, J.M., Fagan, B., van Maanen, A., Cooke, B.M., Doohan, F.M., 2003. Studies on *in vitro* growth and pathogenicity of European *Fusarium* fungi. *Eur. J. Plant Pathol.* 109, 577–587. <https://doi.org/10.1023/A:1024712415326>.
- Brown, D.W., Butchko, R.A.E., Busman, M., Proctor, R.H., 2012. Identification of gene clusters associated with fusaric acid, fusarin, and perithecial pigment production in *Fusarium verticillioides*. *Fungal Biol.* 49, 521–532. <https://doi.org/10.1016/j.fgb.2012.05.010>.

- Cambaza, E., 2018. Comprehensive description of *Fusarium graminearum* pigments and related compounds. *Foods* 7, 165. <https://doi.org/10.3390/foods7100165>.
- Carroll, A.M., Sweigard, J.A., Valent, B., 1994. Improved vectors for selecting resistance to hygromycin. *Fungal Genet Rep* 41, 5. <https://doi.org/10.4148/1941-4765.1367>.
- Christensen, R., 1997. Multiple comparisons: theory and methods. *Technometrics* 39, 232–233. <https://doi.org/10.1080/00401706.1997.10485097>.
- Covert, S.F., Kapoor, P., Lee, M., Briley, A., Nairn, C.J., 2001. *Agrobacterium tumefaciens*-mediated transformation of *Fusarium circinatum*. *Mycol. Res.* 105, 259–264. <https://doi.org/10.1017/S0953756201003872>.
- De Vos, L., van der Nest, M.A., van der Merwe, N.A., Myburg, A.A., Wingfield, M.J., Wingfield, B.D., 2011. Genetic analysis of growth, morphology and pathogenicity in the F1 progeny of an interspecific cross between *Fusarium circinatum* and *Fusarium subglutinans*. *Fungal Biol.* 115, 902–908. <https://doi.org/10.1016/j.funbio.2011.07.003>.
- De Vos, L., van der Nest, M.A., Santana, Q.C., van Wyk, S., Leeuwendaal, K.S., Wingfield, B.D., Steenkamp, E.T., 2024. Chromosome-level assemblies for the pine pitch canker pathogen *Fusarium circinatum*. *Pathogens* 13, 70. <https://doi.org/10.3390/pathogens13010070>.
- De Wit, P.J.G.M., 2016. Apoplastical fungal effectors in historic perspective; a personal view. *New Phytol.* 212, 805–813. <https://doi.org/10.1111/nph.14144>.
- Doohan, F.M., Brennan, J., Cooke, B.M., 2003. Influence of climatic factors on *Fusarium* species pathogenic to cereals. In: *Epidemiology of Mycotoxin Producing Fungi*. Springer, Netherlands, Dordrecht, pp. 755–768. [https://doi.org/10.1007/978-94-017-1452-5\\_10](https://doi.org/10.1007/978-94-017-1452-5_10).
- Doudna, J.A., Charpentier, E., 2014. The new frontier of genome engineering with CRISPR-Cas9. *Science* 346, 6213. <https://doi.org/10.1126/science.1258096>.
- Drenkhan, R., Ganley, B., Martín-García, J., Vahalík, P., Adamson, K., Adamčíková, K., Ahumada, R., Blank, L., Bragança, H., Capretti, P., Cleary, M., Corneo, C., Davydenko, K., Diez, J.J., Lehtijärvi, H.T.D., Dvorák, M., Enderle, R., Fourie, G., Georgieva, M., Ghelardini, L., Hantula, J., Ios, R., Iturriza, E., Kanetis, L., Karpun, N.N., Koltay, A., Landera, S., Markovskaja, S., Mesanza, N., Milenkovic, I., Musolin, D.L., Nikolaou, K., Nowakowska, J.A., Ogris, N., Oskay, F., Ozasko, T., Papazova-Anakieva, I., Paraschiv, M., Pasquali, M., Pecori, F., Rafoss, T., Raitelaityte, K., Raposo, R., Robin, C., Rodas, C.A., Santini, A., Sanz-Ros, A.V., Selikhovkin, A.V., Solla, A., Soukainen, M., Soulioti, N., Steenkamp, E.T., Tsopeles, P., Vemic, A., Vettraino, A.M., Wingfield, M.J., Woodward, S., Zamora-Ballesteros, C., Mullett, M.S., 2020. Global geographic distribution and host range of *Fusarium circinatum*, the causal agent of pine pitch canker. *Forests* 11, 724. <https://doi.org/10.3390/F11070724>.
- Dvorák, M., Janoš, P., Botella, L., Rotková, G., Zas, R., 2017. Spore dispersal patterns of *Fusarium circinatum* on an infested Monterey pine forest in North-Western Spain. *Forests* 8 (11), 432. <https://doi.org/10.3390/f8110432>.
- Egorov, A.A., Alexandrov, A.I., Urakov, V.N., Makeeva, D.S., Edakin, R.O., Kuschchenko, A.S., Gladyshev, V.N., Kulakovskiy, I.V., Dmitriev, S.E., 2021. A standard knockout procedure alters expression of adjacent loci at the translational level. *Nucleic Acids Res.* 49, 11134–11144. <https://doi.org/10.1093/nar/gkab872>.
- Ferrara, M., Haidukowski, M., Logrieco, A.F., Leslie, J.F., Mulé, G., 2019. A CRISPR-Cas9 system for genome editing of *Fusarium proliferatum*. *Sci. Rep.* 9, 19836. <https://doi.org/10.1038/s41598-019-56270-9>.
- Fru, F.F., Steenkamp, E.T., Wingfield, M.J., Santana, Q.C., Roux, J., 2017. Unique clones of the pitch canker fungus, *Fusarium circinatum*, associated with a new disease outbreak in South Africa. *Eur. J. Plant Pathol.* 148, 97–107. <https://doi.org/10.1007/s10658-016-1073-9>.
- Garbelotto, M., Smith, T., Schweigkofler, W., 2008. Variation in rates of spore deposition of *Fusarium circinatum*, the causal agent of pine pitch canker, over a 12-month-period at two locations in northern California. *Phytopathology* 98 (1), 137–143. <https://doi.org/10.1094/PHYTO-98-1-0137>.
- Gordon, T.R., Kirkpatrick, S.C., Aegerter, B.J., Fisher, A.J., Storer, A.J., Wood, D.L., 2011. Evidence for the occurrence of induced resistance to pitch canker, caused by *Gibberella circinata* (anamorph *Fusarium circinatum*), in populations of *Pinus radiata*. *For. Pathol.* 41, 227–232. <https://doi.org/10.1111/j.1439-0329.2010.00678.x>.
- Grigoriev, I.V., Nikitin, R., Haridas, S., Kuo, A., Ohm, R., Otilar, R., Riley, R., Salamov, A., Zhao, X., Korzeniewski, F., Smirnova, T., Nordberg, H., Dubchak, I., Shabalov, I., 2014. MycoCosm portal: gearing up for 1000 fungal genomes. *Nucleic Acids Res.* 42, D699–D704. <https://doi.org/10.1093/nar/gkt1183>.
- Gruber, A.R., Lorenz, R., Bernhart, S.H., Neuböck, R., Hofacker, I.L., 2008. The Vienna RNA websuite. *Nucleic Acids Res.* 36, W70–W74. <https://doi.org/10.1093/nar/gkn188>.
- Guo, L., Wang, J., Liang, C., Yang, L., Zhou, Y., Liu, L., Huang, J., 2022. Fosp9, a novel secreted protein, is essential for the full virulence of *Fusarium oxysporum* f. sp. *cubense* on banana (*Musa* spp.). *Appl. Environ. Microbiol.* 88, e00604–e00621. <https://doi.org/10.1128/aem.00604-21>.
- Hao, G., McCormick, S., Usgaard, T., Tiley, H., Vaughan, M.M., 2020. Characterization of three *Fusarium graminearum* effectors and their roles during *Fusarium* head blight. *Front. Plant Sci.* 11, 579553. <https://doi.org/10.3389/fpls.2020.579553>.
- Hoang, C.X., 2017. The Role of Posttranslational Hypusination of the Eukaryotic Translation Initiation Factor 5A in *Zea mays* and *Fusarium Graminearum*. Unpublished PhD thesis. University of Hamburg.
- Hodge, G.R., Dvorak, W.S., 2000. Differential response of central American and Mexican pine species and *Pinus radiata* to infection by the pitch canker fungus. *New For (Dordr)* 19, 241–258. <https://doi.org/10.1023/A:1006613021996>.
- Jinek, M., Chylinski, K., Fonfara, I., Hauer, M., Doudna, J.A., Charpentier, E., 2012. A programmable dual-RNA-guided DNA endonuclease in adaptive bacterial immunity. *Science* 337, 816–821. <https://doi.org/10.1126/science.1225829>.
- Jones, P., Binns, D., Chang, H.-Y., Fraser, M., Li, W., McAnulla, C., McWilliam, H., Maslen, J., Mitchell, A., Nuka, G., Pesseat, S., Quinn, A.F., Sangrador-Vegas, A., Scheremetjew, M., Yong, S.-Y., Lopez, R., Hunter, S., 2014. InterProScan 5: genome-scale protein function classification. *Bioinformatics* 30, 1236–1240. <https://doi.org/10.1093/bioinformatics/btu031>.
- Josselin, L., Proctor, R.H., Lippolis, V., Cervellieri, S., Hoylaerts, J., De Clerck, C., Fauconnier, M.-L., Moretti, A., 2024. Does alteration of fumonisin production in *Fusarium verticillioides* lead to volatolome variation? *Food Chem.* 438, 138004. <https://doi.org/10.1016/j.foodchem.2023.138004>.
- Kim, S., Park, S.-Y., Kim, K.S., Rho, H.-S., Chi, M.-H., Choi, J., Jongsun, P., Kong, S., Jaejin, P., Goh, J., Lee, Y.-H., 2009. Homeobox transcription factors are required for conidiation and appressorium development in the rice blast fungus *Magnaporthe oryzae*. *PLoS Genet.* 5, e1000757. <https://doi.org/10.1371/journal.pgen.1000757>.
- Kim, K.U., Park, S.K., Kang, S.A., Park, M.K., Cho, M.K., Jung, H.J., Kim, K.Y., Yu, H.S., 2013. Comparison of functional gene annotation of *Toxascaris leonina* and *Toxocara canis* using CLC genomics workbench. *Korean J. Parasitol.* 51, 525–530. <https://doi.org/10.3347/kjp.2013.51.5.525>.
- Kim, S., Kim, D., Cho, S.W., Kim, J., Kim, J.-S., 2014. Highly efficient RNA-guided genome editing in human cells via delivery of purified Cas9 ribonucleoproteins. *Genome Res.* 24, 1012–1019. <https://doi.org/10.1101/gr.171322.113>.
- Kim, H.-S., Lohmar, J.M., Busman, M., Brown, D.W., Naumann, T.A., Divon, H.H., Lysøe, E., Uhlig, S., Proctor, R.H., 2020. Identification and distribution of gene clusters required for synthesis of sphingolipid metabolism inhibitors in diverse species of the filamentous fungus *Fusarium*. *BMC Genomics* 21, 510. <https://doi.org/10.1186/s12864-020-06896-1>.
- Koeck, M., Hardham, A.R., Dodds, P.N., 2011. The role of effectors of biotrophic and hemibiotrophic fungi in infection. *Cell. Microbiol.* 13 (12), 1849–1857. <https://doi.org/10.1111/j.1462-5822.2011.01665.x>.
- Lannou, C., 2012. Variation and selection of quantitative traits in plant pathogens. *Annu. Rev. Phytopathol.* 50, 319–338. <https://doi.org/10.1146/annurev-phyto-081211-173031>.
- Lee, N., Park, J., Kim, J.-E., Shin, J.Y., Min, K., Son, H., 2022. Genome editing using preassembled CRISPR-Cas9 ribonucleoprotein complexes in *Fusarium graminearum*. *PLoS One* 17, e0268855. <https://doi.org/10.1371/journal.pone.0268855>.
- Li, Y., Zheng, X., Zhu, M., Chen, M., Zhang, S., He, F., Chen, X., Lv, J., Pei, M., Zhang, Ye, Zhang, Yunhui, Wang, W., Zhang, J., Wang, M., Wang, Z., Li, G., Lu, G., 2019. MoIVD-mediated leucine catabolism is required for vegetative growth, conidiation and full virulence of the rice blast fungus *Magnaporthe oryzae*. *Front. Microbiol.* 10, 444. <https://doi.org/10.3389/fmicb.2019.00444>.
- Lightfoot, J.D., Fuller, K.K., 2019. CRISPR/Cas9-mediated gene replacement in the fungal keratitis pathogen *Fusarium solani* var. *petroliphilum*. *Microorganisms* 7, 457. <https://doi.org/10.3390/microorganisms7100457>.
- Liu, S., Wu, B., Yang, J., Bi, F., Dong, T., Yang, Q., Hu, C., Xiang, D., Chen, H., Huang, H., Shao, C., Chen, Y., Yi, G., Li, C., Guo, X., 2019. A cerato-platanin family protein FocCP1 is essential for the penetration and virulence of *Fusarium oxysporum* f. sp. *cubense* tropical race 4. *Int. J. Mol. Sci.* 20, 3785. <https://doi.org/10.3390/ijms20153785>.
- Liu, Y., Xin, J., Liu, L., Song, A., Liao, Y., Guan, Z., Fang, W., Chen, F., 2020. Ubiquitin E3 ligase AaBre1 responsible for H2B monoubiquitination is involved in hyphal growth, conidiation and pathogenicity in *Alternaria alternata*. *Genes* 11, 229. <https://doi.org/10.3390/genes11020229>.
- Lu, S., Deng, H., Lin, Y., Huang, M., You, H., Zhang, Y., Zhuang, W., Lu, G., Yun, Y., 2023. A network of sporogenesis-responsive genes regulates the growth, asexual sporogenesis, pathogenesis and fusaric acid production of *Fusarium oxysporum* f. sp. *cubense*. *Journal of Fungi* 10, 1. <https://doi.org/10.3390/jof10010001>.
- Luo, X., Xie, C., Dong, J., Yang, X., Sui, A., 2014. Interactions between *Verticillium dahliae* and its host: vegetative growth, pathogenicity, plant immunity. *Appl. Microbiol. Biotechnol.* 98, 6921–6932. <https://doi.org/10.1007/s00253-014-5863-8>.
- Martín-Rodríguez, N., Sanchez-Zabala, J., Salcedo, I., Majada, J., González-Murua, C., Duñabeitia, M.K., 2015. New insights into radiata pine seedling root infection by *Fusarium circinatum*. *Plant Pathol.* 64, 1336–1348. <https://doi.org/10.1111/ppa.12376>.
- Mitchell, R.G., Steenkamp, E.T., Coutinho, T.A., Wingfield, M.J., 2011. The pitch canker fungus, *Fusarium circinatum*: implications for south African forestry. *South For* 73, 1–13. <https://doi.org/10.2989/20702620.2011.574828>.
- Muñoz-Adalía, E.J., Cañizares, M.C., Fernández, M., Diez, J.J., García-Pedrajas, M.D., 2018. The *Fusarium circinatum* gene *Frho1*, encoding a putative Rho1 GTPase, is involved in vegetative growth but dispensable for pathogenic development. *Forests* 9, 684. <https://doi.org/10.3390/f9110684>.
- Nagy, G., Szebenyi, C., Csereatics, Á., Vaz, A.G., Tóth, E.J., Vágvolgyi, C., Papp, T., 2017. Development of a plasmid free CRISPR-Cas9 system for the genetic modification of *Mucor circinelloides*. *Sci. Rep.* 7, 16800. <https://doi.org/10.1038/s41598-017-17118-2>.
- Nirenberg, H.L., O'Donnell, K., 1998. New *Fusarium* species and combinations within the *Gibberella fujikuroi* species complex. *Mycologia* 90, 434–458.
- Pariaud, B., Ravigné, V., Halkett, F., Goyeau, H., Carlier, J., Lannou, C., 2009. Aggressiveness and its role in the adaptation of plant pathogens. *Plant Pathology* 58, 409–424. <https://doi.org/10.1111/j.1365-3059.2009.02039.x>.
- Phasha, M.M., Wingfield, M.J., Wingfield, B.D., Coetzee, M.P.A., Hallen-Adams, H., Fru, F., Swalarsk-Parry, B.S., Yilmaz, N., Duong, T.A., Steenkamp, E.T., 2021a. Ras2 is important for growth and pathogenicity in *Fusarium circinatum*. *Fungal Biol.* 150, 103541. <https://doi.org/10.1016/j.fgb.2021.103541>.
- Phasha, M.M., Wingfield, B.D., Wingfield, M.J., Coetzee, M.P.A., Hammerbacher, A., Steenkamp, E.T., 2021b. Deciphering the effect of FUB1 disruption on fusaric acid production and pathogenicity in *Fusarium circinatum*. *Fungal Biol.* 125, 1036–1047. <https://doi.org/10.1016/j.funbio.2021.07.002>.

- Plett, J.M., Plett, K.L., 2022. Leveraging genomics to understand the broader role of fungal small secreted proteins in niche colonization and nutrition. *ISME Communications* 2, 49. <https://doi.org/10.1038/s43705-022-00139-y>.
- Pokhrel, A., Seo, S., Wang, Q., Coleman, J.J., 2022. Targeted gene disruption via CRISPR/Cas9 ribonucleoprotein complexes in *Fusarium oxysporum*. In: Coleman, J. (Ed.), *Fusarium Wilt. Methods in Molecular Biology*, vol. 2391. Humana, New York, NY, pp. 75–87. [https://doi.org/10.1007/978-1-0716-1795-3\\_7](https://doi.org/10.1007/978-1-0716-1795-3_7).
- Rodríguez-Ortiz, R., Limón, M.C., Avalos, J., 2013. Functional analysis of the *carS* gene of *Fusarium fujikuroi*. *Mol. Genet. Genomics* 288, 157–173.
- Santana, Q.C., Coetzee, M.P.A., Wingfield, B.D., Wingfield, M.J., Steenkamp, E.T., 2016. Nursery-linked plantation outbreaks and evidence for multiple introductions of the pitch canker pathogen *Fusarium circinatum* into South Africa. *Plant Pathol* 65, 357–368. <https://doi.org/10.1111/ppa.12437>.
- Savojardo, C., Martelli, P.L., Fariselli, P., Profiti, G., Casadio, R., 2018. BUSCA: an integrative web server to predict subcellular localization of proteins. *Nucl. Acids Res* 46, W459–W466. <https://doi.org/10.1093/nar/gky320>.
- Schweigkofler, W., O'Donnell, K., Garbelotto, M., 2004. Detection and quantification of airborne conidia of *Fusarium circinatum*, the causal agent of pine pitch canker, from two California sites by using a real-time PCR approach combined with a simple spore trapping method. *Appl. Environ. Microbiol.* 70, 3512–3520. <https://doi.org/10.1128/AEM.70.6.3512-3520.2004>.
- Shinkado, S., Saito, H., Yamazaki, M., Kotera, S., Arazoe, T., Arie, T., Kamakura, T., 2022. Genome editing using a versatile vector-based CRISPR/Cas9 system in *Fusarium* species. *Sci. Rep.* 12, 16243. <https://doi.org/10.1038/s41598-022-20697-4>.
- Smulian, A.G., Gibbons, R.S., Demland, J.A., Spaulding, D.T., Deepe, G.S., 2007. Expression of hygromycin phosphotransferase alters virulence of *Histoplasma capsulatum*. *Eukaryot. Cell* 6, 2066–2071. <https://doi.org/10.1128/EC.00139-07>.
- Song, R., Zhai, Q., Sun, L., Huang, E., Zhang, Y., Zhu, Y., Guo, Q., Tian, Y., Zhao, B., Lu, H., 2019. CRISPR/Cas9 genome editing technology in filamentous fungi: progress and perspective. *Appl. Microbiol. Biotechnol.* 103, 6919–6932. <https://doi.org/10.1007/s00253-019-10007-w>.
- Spersneider, J., Dodds, P.N., 2022. EffectorP 3.0: prediction of apoplastic and cytoplasmic effectors in fungi and oomycetes. *Mol. Plant Microbe Interact.* 35, 146–156. <https://doi.org/10.1094/MPMI-08-21-0201-R>.
- Spersneider, J., Gardiner, D.M., Dodds, P.N., Tini, F., Covarelli, L., Singh, K.B., Manners, J.M., Taylor, J.M., 2016. Effector P: predicting fungal effector proteins from secretomes using machine learning. *New Phytol.* 210, 743–761. <https://doi.org/10.1111/nph.13794>.
- Studt, L., Wiemann, P., Kleigrew, K., Humpf, H.-U., Tudzynski, B., 2012. Biosynthesis of fusarubins accounts for pigmentation of *Fusarium fujikuroi* perithecia. *Appl. Environ. Microbiol.* 78, 4468–4480. <https://doi.org/10.1128/AEM.00823-12>.
- Swalarsk-Parry, B.S., De Vos, L., Fru, F.F., Santana, Q.C., van der Nest, M.A., Wingfield, B.D., Wingfield, M.J., Herron, D.A., Ramaswe, J.B., Dewing, C., Sayari, M., 2024. Wide variation in aggressiveness and growth in south African *Fusarium circinatum* isolates with geographical origin as the primary determinant. *South. For. J. For. Sci.* 86 (3), 214–221.
- Swett, C.L., Kirkpatrick, S.C., Gordon, T.R., 2016. Evidence for a hemibiotrophic association of the pitch canker pathogen *Fusarium circinatum* with *Pinus radiata*. *Plant Dis.* 100, 79–84. <https://doi.org/10.1094/PDIS-03-15-0270-RE>.
- Tanaka, S., Kahmann, R., 2021. Cell wall-associated effectors of plant-colonizing fungi. *Mycologia* 113, 247–260. <https://doi.org/10.1080/00275514.2020.1831293>.
- Tang, L., Yu, X., Zhang, Li, Zhang, Liyuan, Chen, L., Zou, S., Liang, Y., Yu, J., Dong, H., 2020. Mitochondrial FgEch1 is responsible for conidiation and full virulence in *Fusarium graminearum*. *Curr. Genet.* 66, 361–371. <https://doi.org/10.1007/s00294-019-01028-z>.
- Teufel, F., Almagro Armenteros, J.J., Johansen, A.R., Gíslason, M.H., Pihl, S.I., Tsirigos, K.D., Winther, O., Brunak, S., von Heijne, G., Nielsen, H., 2022. SignalP 6.0 predicts all five types of signal peptides using protein language models. *Nat. Biotechnol.* 40, 1023–1025. <https://doi.org/10.1038/s41587-021-01156-3>.
- Teulet, A., Quan, C., Evangelisti, E., Wanke, A., Yang, W., Schornack, S., 2023. A pathogen effector FOLD diversified in symbiotic fungi. *New Phytol.* 239, 1127–1139. <https://doi.org/10.1111/nph.18996>.
- Turgeon, B.G., Condon, B., Liu, J., Zhang, N., 2010. Protoplast transformation of filamentous fungi. Sharon, A. (eds) *molecular and cell biology methods for fungi*. Methods in Molecular Biology 638, 3–19. [https://doi.org/10.1007/978-1-60761-611-5\\_1](https://doi.org/10.1007/978-1-60761-611-5_1).
- Ullah, M., Xia, L., Xie, S., Sun, S., 2020. CRISPR/Cas9-based genome engineering: a new breakthrough in the genetic manipulation of filamentous fungi. *Biotechnol. Appl. Biochem.* 67 (6), 835–851. <https://doi.org/10.1002/bab.2077>.
- van der Does, H.C., Rep, M., 2017. Adaptation to the host environment by plant-pathogenic fungi. *Annu. Rev. Phytopathol.* 55 (1), 427–450.
- Visser, E.A., Wegryzn, J.L., Steenkamp, E.T., Myburg, A.A., Naidoo, S., 2019. Dual rna-seq analysis of the pine-*Fusarium circinatum* interaction in resistant (*Pinus tecunumanii*) and susceptible (*Pinus patula*) hosts. *Microorganisms* 7, 315. <https://doi.org/10.3390/microorganisms7090315>.
- Wang, Q., Coleman, J.J., 2019a. Progress and challenges: development and implementation of CRISPR/Cas9 technology in filamentous fungi. *Computational Structural Biotechnology J* 17, 761–769. <https://doi.org/10.1016/j.csbj.2019.06.007>.
- Wang, Q., Coleman, J.J., 2019b. CRISPR/Cas9-mediated endogenous gene tagging in *Fusarium oxysporum*. *Fungal Biol.* 126, 17–24. <https://doi.org/10.1016/j.fgb.2019.02.002>.
- Wang, Q., Cobine, P.A., Coleman, J.J., 2018a. Efficient genome editing in *Fusarium oxysporum* based on CRISPR/Cas9 ribonucleoprotein complexes. *Fungal Genet. Biol.* 117, 21–29. <https://doi.org/10.1016/j.fgb.2018.05.003>.
- Wang, Z., Gudibanda, A., Ugwuowo, U., Trail, F., Townsend, J.P., 2018b. Using evolutionary genomics, transcriptomics, and systems biology to reveal gene networks underlying fungal development. *Fungal Biol. Rev.* 32, 249–264. <https://doi.org/10.1016/j.fbr.2018.02.001>.
- Wang, C., Wang, P., Han, S., Wang, L., Zhao, Y., Juan, L., 2020. FunEffector-Pred: identification of fungi effector by activate learning and genetic algorithm sampling of imbalanced data. *IEEE Access* 8, 57674–57683. <https://doi.org/10.1109/ACCESS.2020.2982410>.
- Wang, Y., Zhang, X., Wang, T., Zhou, S., Liang, X., Xie, C., Kang, Z., Chen, D., Zheng, L., 2022. The small secreted protein FoSp1 elicits plant defenses and negatively regulates pathogenesis in *Fusarium oxysporum* f. sp. *cubense* (Foc4). *Front. Plant Sci.* 13. <https://doi.org/10.3389/fpls.2022.873451>.
- Wilson, A.M., Wingfield, B.D., 2020. CRISPR-Cas9-mediated genome editing in the filamentous ascomycete *Huntia omanensis*. *J. Vis. Exp.* 8, 15. <https://doi.org/10.3791/61367>.
- Wingfield, M.J., Hammerbacher, A., Ganley, R.J., Steenkamp, E.T., Gordon, T.R., Wingfield, B.D., Coutinho, T.A., 2008. Pitch Canker Caused by *Fusarium circinatum* - a Growing Threat to Pine Plantations and Forests Worldwide. *Plant Pathol., Australas.* <https://doi.org/10.1017/AP08036>.
- Wingfield, B.D., Liu, M., Nguyen, H.D.T., Lane, F.A., Morgan, S.W., De Vos, L., Wilken, P. M., Duong, T.A., Aylward, J., Coetzee, M.P.A., Dadej, K., De Beer, Z.W., Findlay, W., Havenga, M., Kolarik, M., Menzies, J.G., Naidoo, K., Pochopski, O., Shoukouhi, P., Santana, Q.C., Seifert, K.A., Soal, N., Steenkamp, E.T., Tatham, C.T., van der Nest, M. A., Wingfield, M.J., 2018. Nine draft genome sequences of *Claviceps purpurea* s.lat., including *C. Arundinis*, *C. Humidiphila*, and *C. Cf. spartinae*, pseudomolecules for the pitch canker pathogen *Fusarium circinatum*, draft genome of *Davidsoniella eucalypti*, *Grossmannia galeiformis*, *Quambalaria eucalypti*, and *Teratosphaeria destructans*. *IMA Fungus* 9, 401–418. <https://doi.org/10.5598/imafungus.2018.09.02.10>.
- Xiong, D., Wang, Y., Tian, C., 2019. A novel gene from a secondary metabolism gene cluster is required for microsclerotia formation and virulence in *Verticillium dahliae*. *Phytopathology Research* 1, 31. <https://doi.org/10.1186/s42483-019-0039-1>.
- Yang, C., Sun, J., Wu, Z., Jiang, M., Li, D., Wang, X., Zhou, C., Liu, X., Ren, Z., Wang, J., Sun, M., Sun, W., Gao, J., 2023. FoRSR1 is important for conidiation, fusaric acid production, and pathogenicity in *Fusarium oxysporum* f. sp. *ginseng*. *Phytopathology* 113, 1244–1253. <https://doi.org/10.1094/PHYTO-10-22-0372-R>.
- Zhao, C., Fraczek, M.G., Dineen, L., Lebedinec, R., Macheleidt, J., Heinekamp, T., Delneri, D., Bowyer, P., Brakhage, A.A., Bromley, M., 2019. High-throughput gene replacement in *Aspergillus fumigatus*. *Curr. Protoc. Microbiol.* 54, e88. <https://doi.org/10.1002/cpmc.88>.
- Zheng, Y.-M., Lin, F.-L., Gao, H., Zou, G., Zhang, J.-W., Wang, G.-Q., Chen, G.-D., Zhou, Z.-H., Yao, X.-S., Hu, D., 2017. Development of a versatile and conventional technique for gene disruption in filamentous fungi based on CRISPR-Cas9 technology. *Sci. Rep.* 7, 9250. <https://doi.org/10.1038/s41598-017-10052-3>.